Crystal structure, Raman spectroscopy, far-infrared, and microwave dielectric properties of $(1-x)La(MgSn)_{0.5}O_3-xNd(MgSn)_{0.5}O_3$ system

G. Santosh Babu,[1] V. Subramanian,[1,a)] V. R. K. Murthy,[1] R. L. Moreira,[2] and R. P. S. M. Lobo[3]
[1]*Department of Physics, Indian Institute of Technology-Madras, Chennai 600 036, India*
[2]*Departamento de Física, ICEx, UFMG, CP 702, Belo Horizonte, Minas Gerais 30123-970, Brazil*
[3]*Laboratoire Photons et Matière (CNRS–UPR5), ESPCI, Université Pierre et Marie Curie, 10 rue Vauquelin, 75231 Paris Cedex 05, France*

(Received 13 November 2007; accepted 22 January 2008; published online 18 April 2008)

The complex perovskite system $(1-x)La(MgSn)_{0.5}O_3-xNd(MgSn)_{0.5}O_3$ with the composition $(x=0-1)$ was prepared by the solid state reaction method. Structural and spectroscopic studies were carried out to understand the variation of dielectric properties with x. Rietveld refinement was carried out with the initial model obtained by using the structure prediction and diagnostic software. The symmetry of the compositions was determined to be monoclinic with space group $P2_1/n$, which corresponds to the $a^-a^-c^+$ tilting system, and the long-range order parameter was found to decrease with an increase in neodymium concentration. Raman spectra were analyzed by fitting the A_{1g}-like mode to a Lorentzian peak shape. Intrinsic dielectric parameters were estimated by fitting infrared reflectance spectra with the four-parameter semiquantum model. Transverse optic phonon mode strengths and average phonon damping were calculated. The origin of increase in the intrinsic loss with the composition variation is discussed. Microwave measurements were carried out in the frequency range of 9–11 GHz. The dielectric constant decreases and the temperature coefficient of resonant frequency becomes less negative with the increase in neodymium concentration. © *2008 American Institute of Physics*. [DOI: 10.1063/1.2902932]

I. INTRODUCTION

The rapid growth of wireless communications and information access in the last decade stimulated research on microwave dielectrics, which are used in handsets and base station circuits.[1] High dielectric constant (ε'), high quality factor (Q), and near zero temperature coefficient of resonant frequency (τ_f) are the three prerequisites for a material to be useful in those applications. In particular, base station manufacturer requires moderately high dielectric constant, low cost, and high Q materials.[1] Recently, rare earth (RE)-based complex perovskites with the chemical formula $RE(B'B'')O_3$ have received considerable attention as potential candidates for dielectric resonators and as an alternative to the expensive tantalum and niobium based perovskites.[2–4] The tolerance factor (t) of these RE-based perovskites is smaller than 1, which facilitates the tilting of BO_6 octahedrons. These materials are known to exhibit $P2_1/n$ symmetry with $a^-a^-c^+$ tilting. The monoclinic $P2_1/n$ symmetry supports the 1:1 chemical ordering, whereas the symmetry becomes orthorhombic $Pbnm$ for the disordered structure.[5,6] In ABX_3 perovskites, the A-site cation lies on the mirror plane in $Pbnm$ setting with the position $(x, y, 0.25)$. The different identities and sizes of the B-site cations in $P2_1/n$ destroy the strict symmetry of the mirror plane that result in a slight deviation of the z coordinate of the A-site cation from 0.25.[7,8]

Chemical structure, cation ordering, microstructure, constituent ions, and phonon characteristics are the various factors that influence the microwave dielectric properties. In particular, the dielectric loss in ceramics is known to be caused by both extrinsic factors (porosity, impurities, etc.) and intrinsic losses (lattice absorption due to crystal anharmonicity).[9] Optimization of all the properties is a challenging task. Reaney *et al.*[10] have shown that a decrease in the tolerance factor results in a decrease in the temperature coefficient of the resonant frequency in alkaline earth complex perovskites. However, $Nd(MgTi)_{0.5}O_3$ (NMT) with a tolerance factor (t) of 0.92 [smaller than that of $La(MgTi)_{0.5}O_3$ (LMT) with $t=0.95$] is shown to possess a less negative temperature coefficient of resonant frequency.[3,11] First principles calculations on $CaTiO_3$ and $Ca(AlNb)_{0.5}O_3$ reveal that the differences in the properties of low frequency polar phonons correlate with the temperature coefficient of resonant frequency and permittivity.[12]

Spectroscopic techniques give the advantage of studying phonon modes and thereby enable better understanding of the dielectric properties. The structural modifications, qualitative analysis of long range order (LRO), and distortions in the octahedra can be studied by using Raman spectroscopy.[13,14] Runka *et al.*[13] concluded that the cubic F_{2g} mode splits into doublets and triplets with the lowering of the symmetry, while the sharpness and intensity of the F_{2g} and A_{1g} modes varied with the variation in the ordering.

Infrared (IR) reflectivity is highly sensitive to the degree of order in a material.[15] Intrinsic properties and average phonon damping can be estimated by fitting the reflectivity data to the four-parameter semiquantum model.[2] IR reflectivity is not so sensitive to the details of processing and to small

a)Author to whom correspondence should be addressed. Tel.: +91-44-22574883. FAX: +91-44-22570545. Electronic mail: manianvs@iitm.ac.in.

concentration (of the order of 1 wt %) of dopants.[16] The IR-active modes corresponding to $A-BO_6$ vibration are shown to be responsible for the main contribution of dielectric properties in the solid solution of LMT-NMT.[3] Recently, a combined study of Raman and Fourier transform infrared (FTIR) on $La(Mg_{0.5}Ti_{(0.5-x)}Sn_x)O_3$ concluded that the dielectric loss strongly correlates with the variation in the LRO.[2]

This work reports on the structure and characterization of the $(1-x)La(MgSn)_{0.5}O_3-xNd(MgSn)_{0.5}O_3$ system. The structure of the compounds is determined and LRO is estimated by using Rietveld refinement of the x-ray diffraction data. The initial model for the refinement is obtained by using the "structure prediction and diagnostic software" (SPUDS).[8] It was previously shown that SPUDS predicts the structures of perovskite materials with good accuracy.[17] This paper also investigates the Raman, IR, and microwave dielectric properties of the ceramics. The variation of the LRO with the composition is analyzed by using Raman spectroscopy. Intrinsic dielectric parameters are obtained by extrapolating IR fitting values to microwave frequencies. Correlation of the dielectric properties with the LRO and phonon characteristics is discussed.

II. EXPERIMENT

The $(1-x)La(MgSn)_{0.5}O_3-xNd(MgSn)_{0.5}O_3$ ($x=0.0$, 0.25, 0.5, 0.75, and 1.0) powders were prepared by the solid state reaction method by mixing individual high-purity oxides La_2O_3 (Alfa Aesar, 99.99%), MgO (Alfa Aesar, 99.95%), Nd_2O_3 (Alfa Aesar, 99.9%), and SnO_2 (Alfa Aesar, 99.9%). The starting materials were stoichiometrically weighed after drying La_2O_3 and Nd_2O_3 at 1000 °C for 24 h and MgO at 800 °C for 6 h to remove moisture content and carbonates. The powders were then dry mixed with an agate mortar and pestle and subsequently wet mixed by using distilled water. Each wet mixed powder was dried in an oven at 150 °C for 6 h. The calcination temperature was varied between 1150 and 1200 °C with a duration of 3–5 h. The calcined powder with the organic binder polyvinyl alcohol was pressed into pellets by using a uniaxial press and the binder was evaporated at 500 °C for 12 h. Sintering was carried out at 1600 °C for 5 h.

X-ray diffraction data were collected by using PaNAlytical X'pert pro MPD in Bragg–Brentano geometry with an X'celerator detector. The collection conditions were Cu Kα radiation, 40 kV, 30 mA, 0.033° step scan, 1.0° divergence slit, and 0.02 rad incident and receiving soller slits. Rietveld refinement was performed by using the GSAS suite with EXPGUI.[18,19] Shifted Chebyschev with nine terms was used to describe the background. A pseudo-Voigt (profile function 3 in GSAS) was used to model the peak shapes.

The samples were one side polished by using 0.25 μm diamond paste and subsequently annealed at 500 °C for 8 h to remove the residual stress for spectroscopic measurements. Raman measurements were carried out by using a Horiba Jobin Yvon HR 800 UV Raman spectrometer equipped with a thermoelectrically cooled charge-coupled device. The 632.8 nm line of the He-Ne laser with an output of 10 mW was used as the excitation source and an Olympus BX-41 microscope with a 100× objective was employed for micro-Raman detection. Far-IR and mid-IR reflectance spectra were obtained by using a Bruker IFS 66v FTIR spectrometer. The modulated light beam from the spectrometer was focused onto either the sample or an Au-reference mirror, and the reflected beam was directed onto a 4.2 K bolometer detector (40–650 cm^{-1}) or a DTGS:KBr pyroelectric detector (350–5000 cm^{-1}). The different sources, beam splitters, and detectors used in these studies provided substantial spectral overlap, and the reflectance mismatch between adjacent spectral ranges was less than 1%. The FTIR spectra and the width of the A_{1g} mode of Raman spectra were analyzed by using the FOCUS software.[20] Prior to fitting the A_{1g} mode to the Lorentzian peak, a base line correction was applied to the experimental data.

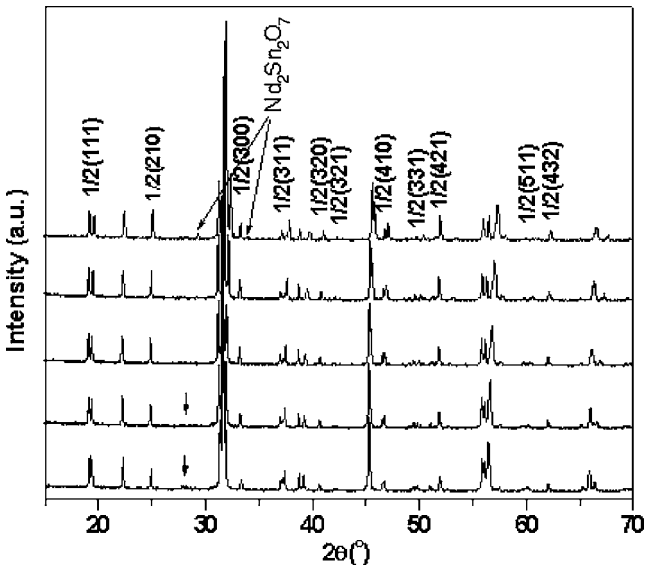

FIG. 1. X-ray diffraction patterns of $(1-x)La(MgSn)_{0.5}O_3-xNd(MgSn)_{0.5}O_3$, $x=0.0$ (bottom), 0.25, 0.5, 0.75, and 1.0 (top) ceramics. The unidentified impurity peak is shown by the arrow mark.

The densities of the sintered samples were measured by using the Archimedes method. The microwave dielectric measurements were carried out by using the N5230A vector network analyzer. The TE_{011} or $TE_{01\delta}$ mode was used for the measurements. The dielectric constant (ε_r) was measured by using the Hakki–Coleman[21] dielectric resonator method, as modified and improved by Courtney.[22] The quality factor (Q) was measured by using the reflection mode gold-coated copper cavity. The temperature coefficient of resonant frequency was measured by using a temperature controlled hot plate enclosure with an invar cavity in the temperature range of 30–70 °C.

III. RESULTS AND DISCUSSION

A. Structure determination

X-ray diffraction patterns of $(1-x)La(MgSn)_{0.5}O_3-xNd(MgSn)_{0.5}O_3$ ($x=0.0$, 0.25, 0.5, 0.75, and 1.0) are presented in Fig. 1. An unidentified impurity peak (<2 wt %) is observed in the $x=0.0$ and $x=0.25$ compositions and a $Nd_2Sn_2O_7$ pyrochlore phase (<2 wt %) is observed in the $x=1.0$ composition. Superlattice reflections corresponding to

TABLE I. Fractional atomic coordinates, thermal parameters, and occupancies of $La(MgSn)_{0.5}O_3$.

	Site	x	y	z	Occupancy	U_{iso} (Å^2)
La	4(e)	0.4885(6)	0.5406(2)	0.2501(3)	1	0.0074(5)
Mg	2(c)	0	0.5	0	0.96	0.006(4)
Mg	2(d)	0.5	0	0	0.04	0.006(4)
Sn	2(d)	0.5	0	0	0.96	0.006(8)
Sn	2(c)	0	0.5	0	0.04	0.006(8)
O	4(e)	0.280(3)	0.282(3)	0.057(3)	1	0.003(3)
O	4(e)	0.210(3)	0.808(3)	0.040(4)	1	0.003(3)
O	4(e)	0.589(2)	−0.024(2)	0.248(3)	1	0.003(3)

Mg/Sn ordering (ooo), in-phase tilting (ooe,oeo,eoo), out-of-phase tilting ($ooo, h+k+l>3$), and A-site cation displacement (eoe,eeo,oee) are observed in all the compositions.[23] All the superlattice reflections are indexed with half integer Miller indices (Fig. 1). The presence of $\frac{1}{2}(111)$ indicates the existence of 1:1 B-site cation ordering in all the compositions.

The high x-ray scattering contrast between Mg^{2+} and Sn^{4+} enables an accurate determination of the cation ordering. All the compositions exhibit monoclinic $P2_1/n$ symmetry. Fractional atomic coordinates, thermal parameters, and occupancies are presented in Tables I–V and the refinement plot for $La(MgSn)_{0.5}O_3$ is shown in Fig. 2. Pyrochlore $Nd_2Sn_2O_7$ is also modeled along with $Nd(MgSn)_{0.5}O_3$ and the fraction of the pyrochlore is determined to be 1 wt %. When the occupancies of the Mg^{2+} and Sn^{4+} sites are refined, the unit cell content is constrained according to the chemical composition. In order to avoid the unwanted correlation with the order parameter, the thermal parameter (U_{iso}) values for the octahedral site are constrained to be equal. The Rietveld discrepancy indices and lattice constants are summarized in Table VI.

Refinement results reveal that the unit cell volume decreases with an increase in neodymium concentration. However, the lattice parameter b is observed to slightly increase with the neodymium concentration. A similar behavior of increase in b is also observed in the $(1-x)La(MgTi)_{0.5}O_3 - xNd(MgTi)_{0.5}O_3$ system.[3] The degree of cation ordering is quantified with the LRO,

$$\mathrm{LRO} = [2(\mathrm{occ})_B - 1] \times 100, \quad (1)$$

where $(occ)_B$ is the fractional occupancy of the B-site cation on the predominantly occupied octahedral site.[24] The LRO of

TABLE II. Fractional atomic coordinates, thermal parameters, and occupancies of $La_{0.75}Nd_{0.25}(MgSn)_{0.5}O_3$.

	Site	x	y	z	Occupancy	U_{iso} (Å^2)
La	4(e)	0.4883(5)	0.5443(2)	0.2504(2)	0.75	0.0093(1)
Nd	4(e)	0.4883(5)	0.5443(2)	0.2504(2)	0.25	0.0093(1)
Mg	2(c)	0	0.5	0	0.96	0.008(5)
Mg	2(d)	0.5	0	0	0.04	0.008(5)
Sn	2(d)	0.5	0	0	0.96	0.008(1)
Sn	2(c)	0	0.5	0	0.04	0.008(1)
O	4(e)	0.292(3)	0.294(3)	0.049(3)	1	0.018(3)
O	4(e)	0.210(3)	0.795(3)	0.045(4)	1	0.018(3)
O	4(e)	0.599(2)	−0.030(2)	0.247(3)	1	0.018(3)

TABLE III. Fractional atomic coordinates, thermal parameters, and occupancies of $La_{0.5}Nd_{0.5}(MgSn)_{0.5}O_3$.

	Site	x	y	z	Occupancy	U_{iso} (Å^2)
La	4(e)	0.4887(6)	0.5474(2)	0.2503(2)	0.5	0.010(11)
Nd	4(e)	0.4887(6)	0.5474(2)	0.2503(2)	0.5	0.010(11)
Mg	2(c)	0	0.5	0	0.95	0.007(5)
Mg	2(d)	0.5	0	0	0.05	0.007(5)
Sn	2(d)	0.5	0	0	0.95	0.007(1)
Sn	2(c)	0	0.5	0	0.05	0.007(1)
O	4(e)	0.297(3)	0.288(3)	0.040(4)	1	0.009(3)
O	4(e)	0.209(3)	0.800(3)	0.051(3)	1	0.009(3)
O	4(e)	0.607(2)	−0.028(2)	0.255(2)	1	0.009(3)

$La(MgSn)_{0.5}O_3$ (LMS) is determined to be 92% and it gradually decreases to 88% for $Nd(MgSn)_{0.5}O_3$ (NMS) .

The extent of B-site cation ordering depends on the difference between the oxidation states of B-site cations, difference between the radii of B-site cations,[7,25] the nature of B'' ion, and the processing conditions.[25] The size difference between Mg^{2+} and Sn^{4+} is 0.03 Å, whereas the size difference between Mg^{2+} and Ti^{4+} is 0.11 Å.[26] Even though the size difference between the B-site cations in the tin based compounds is very small, the LRO observed in the present study is high and is comparable to the LRO observed in $Nd(MgTi)_{0.5}O_3$ (92%).[27] The high degree of LRO may be due to the nature of the Sn^{4+} ion. The main group Sn^{4+} is more electronegative with filled d orbitals, whereas the transition metal Ti^{4+} is less electronegative with empty d orbitals. Barnes[25] observed a high degree of LRO with the main group Sb^{5+} having a high electronegativity compared to the transition metal Ta^{5+} similar to the present work. The high electronegativity of the ion draws the oxygen's electron cloud density toward it effectively compared to the low electronegative ion.[25] The empty d orbitals of Ta^{5+} enable π-bonds with oxygen that stabilize $Ta^{5+}-O-Ta^{5+}$ linkage, whereas Sb^{5+} has no d orbitals that stabilize $Sb^{5+}-O-Sb^{5+}$ linkage.[25,28] Therefore, $Sn^{4+}-O-Sn^{4+}$ bonds are less favorable compared to $Sn^{4+}-O-Mg^{2+}$ bonds. Thus, the cation order minimizes the adjacent Sn^{4+} interactions.

B. Raman spectra

The Raman spectra recorded for the solid solution system are presented in Fig. 3. The predicted Raman-active

TABLE IV. Fractional atomic coordinates, thermal parameters, and occupancies of $La_{0.25}Nd_{0.75}(MgSn)_{0.5}O_3$.

	Site	x	y	z	Occupancy	U_{iso} (Å^2)
La	4(e)	0.4865(5)	0.5510(2)	0.2500(2)	0.25	0.014(5)
Nd	4(e)	0.4865(5)	0.5510(2)	0.2500(2)	0.75	0.014(5)
Mg	2(c)	0	0.5	0	0.94	0.017(7)
Mg	2(d)	0.5	0	0	0.06	0.017(7)
Sn	2(d)	0.5	0	0	0.94	0.017(3)
Sn	2(c)	0	0.5	0	0.06	0.017(3)
O	4(e)	0.293(3)	0.295(3)	0.045(3)	1	0.014(3)
O	4(e)	0.201(3)	0.802(3)	0.052(3)	1	0.014(3)
O	4(e)	0.607(2)	−0.031(2)	0.262(2)	1	0.014(3)

TABLE V. Fractional atomic coordinates, thermal parameters, and occupancies of $Nd(MgSn)_{0.5}O_3$.

	Site	x	y	z	Occupancy	U_{iso} (Å^2)
Nd	4(e)	0.4859(6)	0.5535(2)	0.2502(3)	1	0.012(5)
Mg	2(c)	0	0.5	0	0.94	0.009(2)
Mg	2(d)	0.5	0	0	0.06	0.009(2)
Sn	2(d)	0.5	0	0	0.94	0.009(4)
Sn	2(c)	0	0.5	0	0.06	0.009(4)
O	4(e)	0.298(3)	0.295(3)	0.050(3)	1	0.013(4)
O	4(e)	0.199(3)	0.808(3)	0.061(3)	1	0.013(4)
O	4(e)	0.606(2)	−0.032(2)	0.257(3)	1	0.013(4)

modes for monoclinic $P2_1/n$ space group are 24 ($12A_g+12B_g$).[2] The Raman-active modes for cubic $Fm\bar{3}m$ are ($A_{1g}+2F_{2g}+E_g$). It is worth noticing that B-site 1:1 ordered materials yield structures that proceed from the cubic elpasolite-type structure, which presents four intense Raman-active modes with symmetries $2F_{2g}$, E_g, and A_{1g}.[29] In the low-symmetry structures derived from this cubic phase, the most intense modes will proceed from those of the cubic phase with the pertinent splitting due to the rising of degeneracy. The other modes coming from the activation of silent modes and/or from Brillouin-zone folding due to the increase of the primitive cell volume are usually less intense. According to our previous analysis on $La(Mg_{0.5}Ti_{(0.5-x)}Sn_x)O_3$ ceramics that has the same $P2_1/n$ symmetry,[2] the highest wave number mode (above 650 cm^{-1}) is attributed to the A_{1g}-like mode that corresponds to symmetric breathing of oxygen octahedrons. Modes between 300 and 370 cm^{-1} and the other three in the range of 130–140 cm^{-1} derive from F_{2g} vibrations (A-site cations).

With increasing neodymium concentration (x), the bands do not present the same behavior for frequencies, widths, and intensities. This occurs because some bands are more sensitive to the unit cell volume, others to the tolerance factor, and others to B-site ordering, which have different effects on the bands. Differently, the F_{2g}-like modes in the vicinity of 330 cm^{-1} (associated with movements of A or O ions) tend to merge with increasing x.

Concerning the highest-frequency A_{1g}-like mode (above 650 cm^{-1}), it corresponds to the displacement of oxygen atoms along the $B'-O-B''$ axis. Its frequency is primarily determined by the $B'-O$ and $B''-O$ distances and bonding forces.[30] The full width at half maximum (FWHM) of the A_{1g} mode gives a measure of B-site cation ordering.[2] The Raman shift and FWHM of the A_{1g} mode are summarized in Table VII. The Raman shift gradually decreases with an increase in neodymium concentration, which is attributed to the influence of the A-site ion on the A_{1g} mode and the decrease of the tolerance factor. The FWHM increases with increasing neodymium concentration, which indicates a decrease in the LRO, also in agreement with Rietveld refinement.

TABLE VI. Lattice parameters, Rietveld discrepancy indices, and LRO of the $(1-x)La(MgSn)_{0.5}O_3-xNd(MgSn)_{0.5}O_3$ system.

x	a (Å)	b (Å)	c (Å)	β (deg)	R_{wp} (%)	R_F^2 (%)	χ^2	LRO (%)
0	5.6387(4)	5.7250(4)	8.0219(6)	90.085(3)	6.8	4.9	1.12	92
0.25	5.6140(4)	5.7255(4)	7.9989(5)	90.096(3)	5.8	4.4	1.05	92
0.5	5.5902(4)	5.7292(4)	7.9776(6)	90.123(2)	5.7	4.3	1.10	90
0.75	5.5652(4)	5.7298(4)	7.9533(6)	90.140(2)	5.4	4.2	1.08	88
1	5.5397(3)	5.7304(3)	7.9281(4)	90.155(2)	4.9	4.4	1.04	88

C. FTIR spectra

According to the factor group analysis,[31] the number of IR-active modes for $P2_1/n$ symmetry is 33 ($17A_u+16B_u$). Due to anisotropy averaging out in the ceramic samples, modes A_u and B_u cannot be resolved and, therefore, the number of effective modes would be 17.[2] Figure 4 presents the IR reflectivity spectra of the compositions studied. Modes corresponding to $A-BO_6$ translation modes (vicinity of

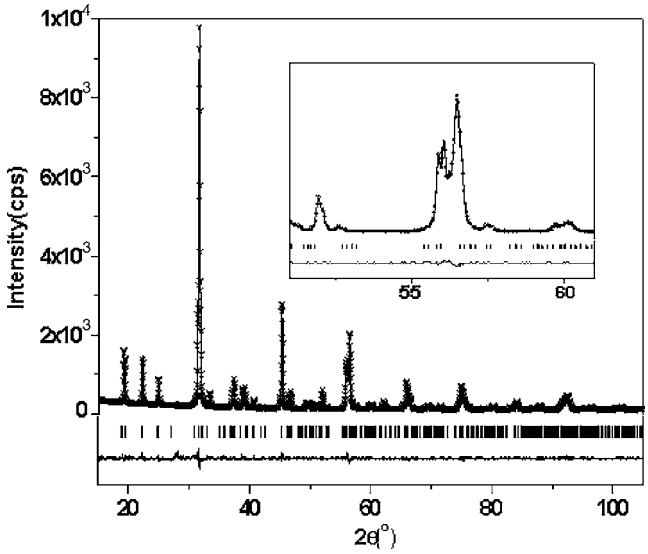

FIG. 2. Final observed (+ marks), calculated (solid line), and difference (below) patterns along with the calculated positions for $La(MgSn)_{0.5}O_3$.

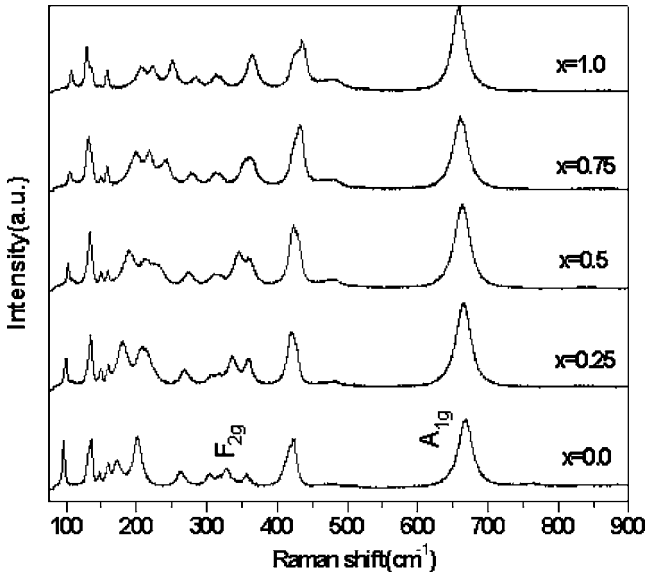

FIG. 3. Raman spectra of the $(1-x)La(MgSn)_{0.5}O_3-xNd(MgSn)_{0.5}O_3$ system.

TABLE VII. Relative densities, dielectric characteristics extrapolated from IR data, Lorentzian fit parameters of the A_{1g} mode (Raman), and dielectric parameters determined at microwave (MW) frequencies for the $(1-x)La(MgSn)_{0.5}O_3-xNd(MgSn)_{0.5}O_3$ system. The uncertainties for ε' and $Q\times f$ are approximately 0.5% and 1%, respectively.

		A_{1g} (Raman)		IR		MW		
Nd concentration (x)	Relative density (%)	Shift (cm^{-1})	FWHM (cm^{-1})	ε'	$Q\times f$ (GHz)	ε'	$Q\times f$ (GHz)	τ_f (ppm/°C)
0.0	98.4	667.7	24.0	19.1	123 600	19.8	75 000	−82
0.25	97.8	665.0	24.4	18.9	105 800	19.5	68 000	−75
0.5	97.6	663.2	24.9	18.5	102 900	19.4	64 000	−66
0.75	98.2	661.1	25.2	18.3	99 700	19.2	70 000	−60
1.0	98.5	658.5	25.4	18.0	93 900	19.1	68 000	−53

150 cm^{-1}), $B-O-B$ stretching modes (200–500 cm^{-1}), and $B-O_6$ bending modes (500–800 cm^{-1}) (Ref. 2) are present in all the compositions. Modes between 200 and 500 cm^{-1} reconfirm the existence of cation ordering and tilting in all the compositions. It is also observed that the mode in the vicinity of 350 cm^{-1} broadens with an increase in neodymium concentration, suggesting a decrease in LRO.

In order to determine the intrinsic parameters, mode strengths, and average phonon damping, reflectivity spectra are fitted to a four-parameter model. All the compositions are fitted with 17 modes. The estimated intrinsic values of the dielectric constant and quality factor are listed in Table VII. Figure 5 presents the TO mode frequencies and strengths and their variations with neodymium concentration (full squares denote the strength of the TO modes). The intrinsic dielectric constant slightly decreases with the increase in neodymium concentration. The slight variation is due to the variation in mode strengths in the range of 150–175 cm^{-1} and, therefore, the modes corresponding to $A-BO_6$ vibrations are responsible for the decrease in the dielectric constant. Higher strength of $A-BO_6$ modes and the mode at 350 cm^{-1} is in accordance with the previous studies.[2,3]

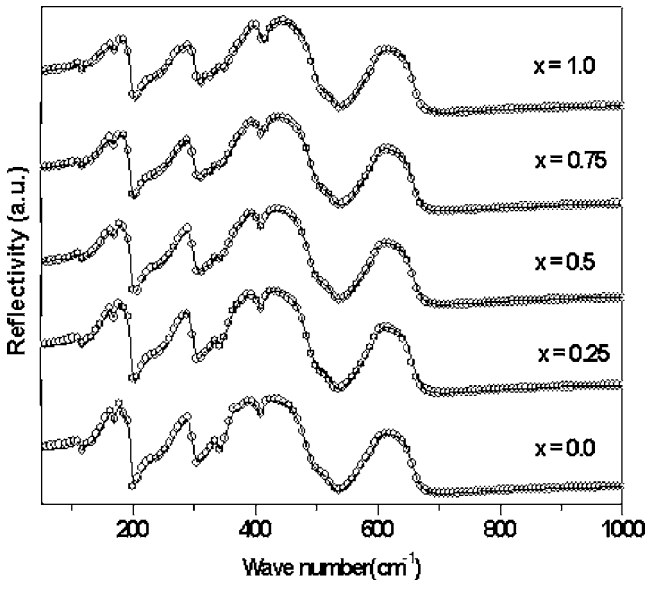

FIG. 4. IR reflectivity spectra of the $(1-x)La(MgSn)_{0.5}O_3-xNd(MgSn)_{0.5}O_3$ perovskite system (open circles represent the experimental data and continuous line represents the fitted model).

Figure 6 presents the variation in average phonon damping,[2] $\langle\gamma(TO)\rangle$, and intrinsic Q as function of tin concentration,

$$\langle\gamma(TO)\rangle = \frac{\Sigma_{j=1}^{n}\gamma_j(TO)\Delta\varepsilon_j}{\Sigma_{j=1}^{n}\Delta\varepsilon_j}, \tag{2}$$

where γ_j and $\Delta\varepsilon_j$ represent damping and dielectric strength of the TO mode, respectively. The intrinsic Q decreases with the increase in neodymium concentration, whereas the average phonon damping is observed to increase. The increase in phonon damping and decrease in the intrinsic quality factor are attributed to a decrease in LRO.

D. Microwave dielectric properties

Microwave dielectric properties and relative density of $(1-x)La(MgSn)_{0.5}O_3-xNd(MgSn)_{0.5}O_3$ are summarized in Table VII. The dielectric constant slightly decreases with the increase in neodymium concentration, which suggests that neodymium polarizability is smaller than that of lanthanum. The polarizability values (α) reported by Shannon[32] for lanthanum and neodymium are 6.07 and 5.01 $Å^3$, respectively. However, later, the polarizability of lanthanum was revised[33] to 4.82 $Å^3$. This value is smaller than that of neodymium. It

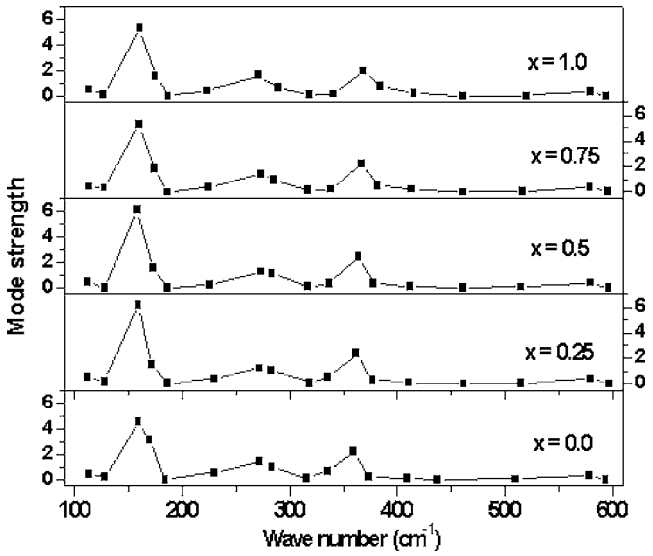

FIG. 5. The variation in TO mode phonon strength as a function of Nd concentration x (open circles represent TO modes).

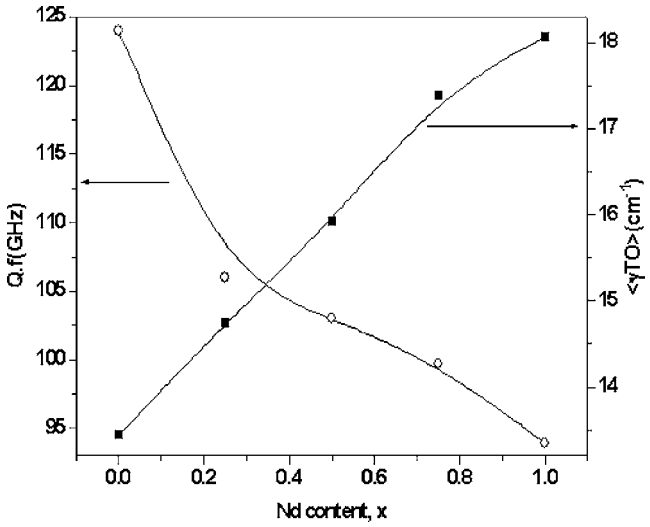

FIG. 6. Intrinsic $Q\times f$ values (open circles) and average TO phonon damping (full squares) as functions of Nd content x.

was shown that in $(1-x)La(MgTi)_{0.5}O_3-xNd(MgTi)_{0.5}O_3$, the dielectric constant also decreases with the increase in neodymium concentration, which is in agreement with the tendency shown in the present study. Indeed, if we revise the ionic polarizabilities for La^{3+} by performing a linear fit of α to the r^3 law for all the series of lanthanide ions (r=ionic radius from Ref. 26, for coordination number CN=8, and α from Ref. 32, except for Ce^{3+}, for which we used 5.47 Å^3, which is also revised after fitting), we found α (La^{3+}) =5.71 Å^3. Now, if we calculate the Clausius–Mossotti dielectric constants for our system, we would have a monotonous decrease such as 26.3 for LMS to 21.7 for NMS, which is in qualitative agreement with our findings and also those of Ref. 3. The lowest experimental values could partially result from some microstructural defects, although the most probable situation is an actual reduction of the ionic effective charges (or polarizabilities) due to partial RE–O covalent bonds, which are similar to $ReTiTaO_6$ compounds.[34]

The microwave quality factors obtained are smaller than the intrinsic values due to extrinsic losses contributed by structural defects. It is well known that $Q\times f$ values also depend on the processing conditions. The extrinsic $Q\times f$ values obtained for x=0.25 and 0.5 compositions are smaller due to the lower relative density of these samples. The temperature coefficient of resonant frequency (τ_f) becomes less negative with the increase in neodymium concentration. However, the tolerance factor decreases with the increase in neodymium concentration. In $(1-x)La(MgTi)_{0.5}O_3-xNd(MgTi)_{0.5}O_3$, a similar behavior is observed,[3] which suggests that τ_f correlates with the nature of the A-site ion. On the other hand, there are very few attempts to relate bond valences of B site ions,[35] covalency of ions with τ_f,[34] and correlation of phonon properties with τ_f by first principles calculations.[12] Detailed studies, viz., first principles calculations and bond valences obtained from accurate bond lengths by neutron diffraction studies, are required to understand the variation in the temperature coefficient of resonant frequency.

IV. CONCLUSIONS

Dense ceramic materials of $(1-x)La(MgSn)_{0.5}O_3-xNd(MgSn)_{0.5}O_3$ are prepared by the solid state reaction method. The structure of the compounds is determined by using Rietveld refinement of x-ray diffraction data. All the compounds exhibit monoclinic $P2_1/n$ with high percentage of B-site cation ordering. Rietveld refinement and FWHM of the A_{1g} mode reveal that LRO decreases with increase in neodymium concentration. The IR modes corresponding to $A-BO_3$ are responsible for the decrease in dielectric constant and the average phonon damping increases with the increase in neodymium concentration. The collective study of Rietveld refinement, Raman spectroscopy, and FTIR spectroscopy reveals that the LRO and intrinsic $Q\times f$ correlate with each other. Microwave dielectric constant and $Q\times f$ decrease with the increase in neodymium concentration. The temperature coefficient of resonant frequency is found to be less negative with the high neodymium concentration.

ACKNOWLEDGMENTS

The authors (G.S.B., V.S., and V.R.K.M.) acknowledge the Council of Scientific and Industrial Research (CSIR), New Delhi, for providing the financial assistance in the form of Sponsored Research Project. R.L.M. acknowledges the Brazilian funding agencies CNPq and Fapemig and the ESPCI for an invited "Chaire Joliot" appointment. The authors would also like to thank Dr. P. N. Santhosh, Department of Physics, IIT Madras, Chennai, India, for the helpful discussions on the x-ray analysis.

[1] I. M. Reaney and D. Iddles, J. Am. Ceram. Soc. **89**, 2063 (2006).
[2] G. Santosh Babu, V. Subramanian, V. R. K. Murthy, I.-N. Lin, C.-T. Chia, and H.-L. Liu, J. Appl. Phys. **102**, 064906 (2007).
[3] M. P. Seabra, A. N. Salak, M. Avdeev, and V. M. Ferreira, J. Phys.: Condens. Matter **15**, 4229 (2003).
[4] R. Ubic, Y. Hu, K. Khamoushi, and I. Abrahams, J. Eur. Ceram. Soc. **26**, 1787 (2006).
[5] M. V. Avdeev, M. P. Seabra, and V. M. Ferreira, J. Mater. Res. **17**, 1112 (2002).
[6] M. V. Avdeev, M. P. Seabra, and V. M. Ferreira, Mater. Res. Bull. **37**, 1459 (2002).
[7] M. T. Anderson, K. B. Greenwood, G. A. Taylor, and K. R. Poeppelmeier, Prog. Solid State Chem. **22**, 197 (1993).
[8] M. W. Lufaso, P. W. Barnes, and P. M. Woodward, Acta Crystallogr. B **62**, 397 (2006).
[9] J. Petzelt and N. Setter, Ferroelectrics **150**, 89 (1993).
[10] I. M. Reaney, E. L. Colla, and N. Setter, Jpn. J. Appl. Phys., Part 1 **33**, 3984 (1994).
[11] S. Y. Cho, C. H. Kim, D. W. Kim, K. S. Hong, and J. H. Kim, J. Mater. Res. **14**, 2484 (1999).
[12] E. Cockayne, J. Appl. Phys. **90**, 1459 (2001).
[13] T. Runka, R. Aleksiyko, M. Berkowski, and M. Drozdowski, Cryst. Res. Technol. **40**, 453 (2005).
[14] R. L. Moreira, F. M. Matinaga, and A. Dias, Appl. Phys. Lett. **78**, 428 (2001).
[15] I. M. Reaney, J. Pezelt, V. V. Voitesekhovskii, F. Chu, and N. Setter, J. Appl. Phys. **76**, 2086 (1994).
[16] J. Petzelt, S. Kamba, G. V. Kozlov, and A. A. Volkov, Ferroelectrics **176**, 145 (1996).
[17] M. W. Lufaso and P. M. Woodward, Acta Crystallogr. B **57**, 725 (2001).
[18] A. C. Lorson and R. B. Von dreele, "General Structure Analysis System (GSAS)," Los Alamos National Laboratory Report No. LAUR 86, 2004.
[19] B. H. Toby, J. Appl. Crystallogr. **34**, 210 (2001).
[20] D. De Sousa Meneses, G. Gruener, M. Malki, and P. Echegut, J. Non-Cryst. Solids **351**, 124 (2005).

[21]B. W. Hakki and P. D. Coleman, IRE Trans. Microwave Theory Tech. **8**, 402 (1960).
[22]W. E. Courtney, IEEE Trans. Microwave Theory Tech. **18**, 476 (1970).
[23]A. M. Glazer, Acta Crystallogr. A **31**, 756 (1975).
[24]C. K. Meghan and P. M. Woodward, J. Solid State Chem. **179**, 1076 (2004).
[25]P. W. Barnes, Ph.D. thesis, The Ohio State University, 2003.
[26]R. D. Shannon, Acta Crystallogr. A **32**, 751 (1976).
[27]W. A. Groen, F. P. F. van Berkel, and D. J. W. Ijdo, Acta Crystallogr. C **42**, 1472 (1986).
[28]P. Woodward, R. D. Hoffmann, and A. W. Slieght, J. Mater. Res. **9**, 2118 (1994).
[29]A. A. Prosandeev, U. Waghmare, I. Levin, and J. Maslar, Phys. Rev. B **71**, 214307 (2005).
[30]M. L. Duyckaerts and P. Tarte, Spectrochim. Acta, Part A **30**, 1171 (1974).
[31]A. P. Ayala, I. Guedes, E. N. Siva, M. S. Augsburger, M. del C. Viola, and J. C. Pedregosa, J. Appl. Phys. **101**, 123511 (2007).
[32]R. D. Shannon, J. Appl. Phys. **73**, 348 (1993).
[33]C. Vineis, P. K. Davies, T. Negas, and S. Bell, Mater. Res. Bull. **31**, 431 (1996).
[34]C. W. A. Paschoal, R. L. Moreira, K. P. Surendran, and M. T. Sebastian, J. Mater. Res. **20**, 1164 (2005).
[35]M. W. Lufaso, Chem. Mater. **16**, 2148 (2004).